

EFFECT OF Scandium and Zirconium ADDITIONS ON CORROSION PROPERTIES OF Al–Mg–Mn Alloy

M. Srinivasa Rao

*Research Scholar, Department of Mechanical Engineering, A.U. College of Engineering (A),
Andhra University, Visakhapatnam, Andhra Pradesh-530003, INDIA*

s2srinu@gmail.com

N. Ramanaiah

*Professor, Department of Mechanical Engineering, A.U. College of Engineering (A), Andhra
University, Visakhapatnam, Andhra Pradesh-530003,INDIA*

n.rchetty1@gmail.com

Abstract

This study investigates the hardness and corrosion resistance of Al–Mg–Mn alloy with minor additions of scandium (Sc) and zirconium (Zr) systematically. Stir casting with cold rolled condition was applied to the four compositions of this alloy, namely Al–4.2Mg–0.6Mn alloy, Al–4.2Mg–0.6Mn–0.2Sc–0.1Zr alloy, Al–4.2Mg–0.6Mn–0.4Sc–0.1Zr alloy, and Al–4.2Mg–0.6Mn–0.6Sc–0.1Zr alloy. Alloying with Sc and Zr has a strong influence on the hardness of Al–Mg–Mn alloys and introduce resistance to corrosion in 3.5wt.% NaCl solution.

Keywords: Al–Mg–Mn–Sc–Zr; hardness; optical microscope; corrosion resistance; scanning electron microscopy; X-ray diffraction

Introduction

The development of light weight metals in the field of engineering and technology is due to the demand for such materials in aerospace, automotive and marine applications. Light weight metals such as aluminium alloys with magnesium and manganese are characterized by a low density and high resistance to corrosion [1, 2].

5XXX series aluminium alloys usually contains Aluminium (Al), Magnesium (Mg) Manganese (Mn) and other metals. Increase in the magnesium content in these 5XXX series alloys leads

to increase in the ultimate tensile strength due to cold working; this involves in decrease in the plastic properties and Manganese and chromium increase in the corrosion resistant and wear resistant respectively [3–4]. However, these elements alone cannot achieve better mechanical properties. For improving these properties on Al–Mg–Mn alloys, investigational studies on adding transition elements of the periodic table like scandium (Sc), zirconium (Zr), hafnium (Hf), and titanium (Ti) etc., to 5XXX series aluminium were begun at the end of the 1960s, specifically on scandium additions [7–8]. From the literature, Al–Sc phase diagram shown in the Fig.1 provides the formation of Al_3Sc phase when Sc addition levels are 0.2wt.% to 0.6wt.%, that is Sc addition levels exceeding the eutectic composition [5–6]. However, Zr is another element for refining the structure of aluminium alloys can reduce the Sc addition levels because Zr shifts the eutectic position to a lower Sc level.

Thus the Al–Mg–Mn alloys, with minor additions of Sc and Zr is a new light-weight structural material, allowing scandium and zirconium unitedly results in $\text{Al}_3\text{Sc}_{1-x}\text{Zr}_x$ phases [9].

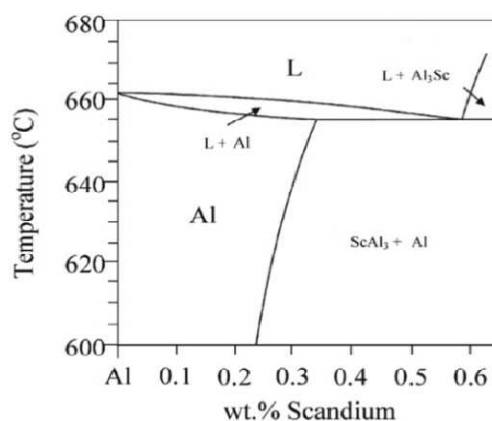


Fig. 1 Al–Sc phase diagram

In the present work an attempt was made to study the effect of systematic addition levels of Sc from (0.2wt.% to 0.6wt.%) with 0.1wt.% Zr to Al–Mg–Mn alloy on mechanical and corrosion properties.

Experimental Methods

• *Materials*

In the present work the four alloys Al–4.2Mg–0.6Mn alloy (hereafter named as specimen–1), Al–4.2Mg–0.6Mn–0.2Sc–0.1Zr alloy (hereafter named as specimen–2), Al–4.2Mg–0.6Mn–0.4Sc–0.1Zr alloy (hereafter named as specimen–3), and Al–4.2Mg–0.6Mn–0.6Sc–0.1Zr

alloy (hereafter named as specimen-4) were produced by melting in an electrical resistance furnace (Fig. 3a). These alloys were prepared by stir casting, using Al-4.2Mg-0.6Mn metal and three master alloys (Al-10wt. %Mg, Al-2wt. %Sc and Al-5wt. %Zr) as shown in the Fig.2(a)–(c), that were melted in alumina crucible and then poured into a metal mould, the casting process as shown in the Fig.3 (a)–(d). The final temperature of the melt was always maintained at $1000 \pm 15^\circ\text{C}$ with the help of the electronic controller. Then the melt was homogenized under stirring at 900°C . Casting was done in cast iron metal mould preheated to 200°C [10–12]. Mould size is 150mm x 150mm x 6mm, then cold-rolled to 5 mm thick sheets. All the alloys were analyzed by spectrochemical methods simultaneously. The chemical compositions of the alloys are given in Table 1. Subsequently, specimens measuring 15 mm in square were prepared for hardness test (Fig.4b), corrosion test (Fig.5b), X-Ray diffraction, optical and scanning electron microscope characterization.



Fig. 2 Master alloys (a) Al-10wt. % Mg (b) Al-2wt. % Sc (c) Al-5wt. % Zr

Table.1 Composition of Modified Al-Mg-Mn Alloy

Alloy type	Mg	Mn	Si	Cr	Zn	Ni	Li	Sc	Zr	Balance
Specimen-1	4.2	0.6	0.17	0.10	0.06	0.006	0.001	–	–	Al
Specimen-2	4.2	0.6	0.17	0.10	0.06	0.006	0.001	0.2	0.1	Al
Specimen-3	4.2	0.6	0.17	0.10	0.06	0.006	0.001	0.4	0.1	Al
Specimen-4	4.2	0.6	0.17	0.10	0.06	0.006	0.001	0.6	0.1	Al

All the specimens were polished with SiC paper and final polish with diamond paste on disc polishing machine. All the polished specimens were cleansed with acetone for microstructural studies [13].



Fig. 3 shows the fabrication process (a) Electrical Resistance Furnace (b) Pouring molten mixture into the preheated permanent mould (c) Al-Mg-Mn-Sc-Zr ascast plate (d) Cold rolling of plate.

- ***Vickers micro hardness measurement***

Hardness of the specimens was measured using a vickers microhardness tester (Fig. 4(a)) and specimens of all four compositions (Fig. 4(b)) with 200 gf load and a dwell time of 15s. Average of five readings were measured and presented.

- ***Microstructure examination***

The surface morphology of the specimens before and after corrosion was examined with an optical microscope and scanning electron microscope. Micro analytical studies were conducted by SEM-EDS.

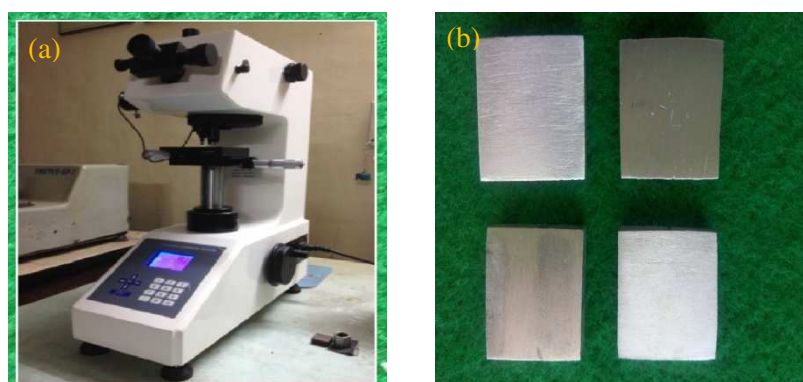


Fig. 4 shows the (a) Vickers's digital microhardness tester (b) specimens for hardness test

- ***X-Ray diffraction Analysis***

X-ray diffraction analysis was carried out to find the presences of different elements in the Al-Mg-Mn-Sc-Zr alloys. It was carried out by X-Ray diffractometer.

- ***Corrosion Measurements***

The corrosion measurements were made according to ASTM G5-87 standards in 3.5 % NaCl solution [14]. Fig.5 (a) and (b) shows the corrosion setup and specimens respectively.

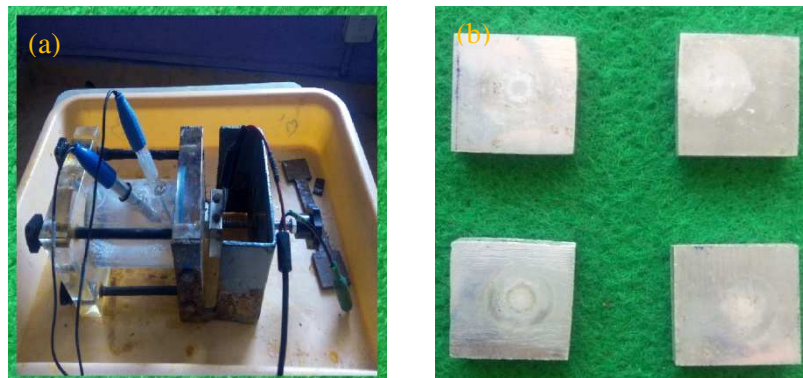


Fig. 5 (a) Corrosion test setup (b) specimens after corrosion test

Results and discussion

- ***Effect of Sc and Zr additions on Hardness***

The influence of Sc and Zr additions on hardness of the Al-Mg-Mn wt. % base alloy is presented in Fig. 6, which reveals significant effect of Sc and Zr additions upon the

hardness of the alloy. This indicates that contribution of Sc and Zr in solid solution strengthening was significant.

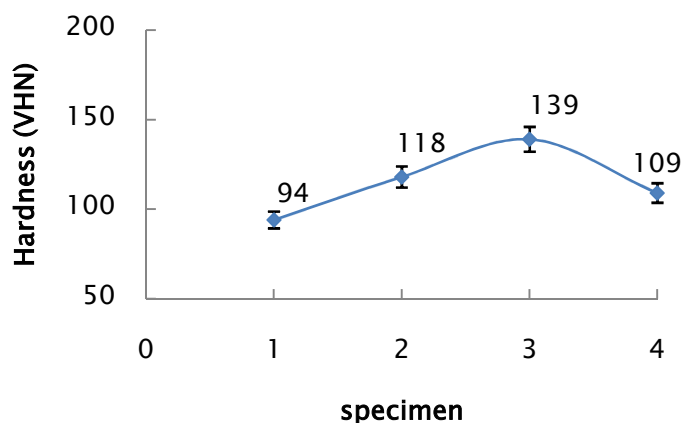


Fig. 6 Vickers hardness measured from specimen-1 to specimen-4.

The hardness of alloys was increased by Sc and Zr additions; however, this effect was significant up to 0.4 wt. % Sc and 0.1wt. % Zr i.e., specimen-3. This gradual increase of hardness was caused by the addition of Sc and Zr apparently, which would have promoted the formation and the dispersion of $Al_3Sc_{1-x}Zr_x$ with the increase of Sc wt. % [15]. The addition of 0.6 wt. % Sc and 0.1 wt. % Zr i.e., specimen-4 lead to a decrease in average hardness by $\sim 15 HV_{0.2}$ [16].

• *Effect of Sc and Zr additions on Microstructure*

The effect of varying amounts of Sc on the phases present in Al-Mg-Mn is presented in Fig. 6. The increasing Sc content leads to the formation of an $Al_3Sc_{1-x}Zr_x$ phase. The phase fraction of the $Al_3Sc_{1-x}Zr_x$ phase increased linearly with Sc content to a maximum of ~ 0.6 wt. %.

The microstructure of the alloys as investigated using optical microscope revealed that Sc addition altered the morphology of intermetallics (Fig. 7). Intermetallics appeared to be fragmented because of the Sc and Zr addition [17].

A higher magnification SEM images of these alloys (specimen-3 to specimen-4) as presented in the Fig. 8 revealed the presence of uniformly distributed particles in Sc and Zr-containing alloys and it convenient to keep scandium and zirconium content levels upto specimen-3 and appearance of non dendrites primary intermetallics observed in the specimen-4 [18], which were not present in the specimen-1.

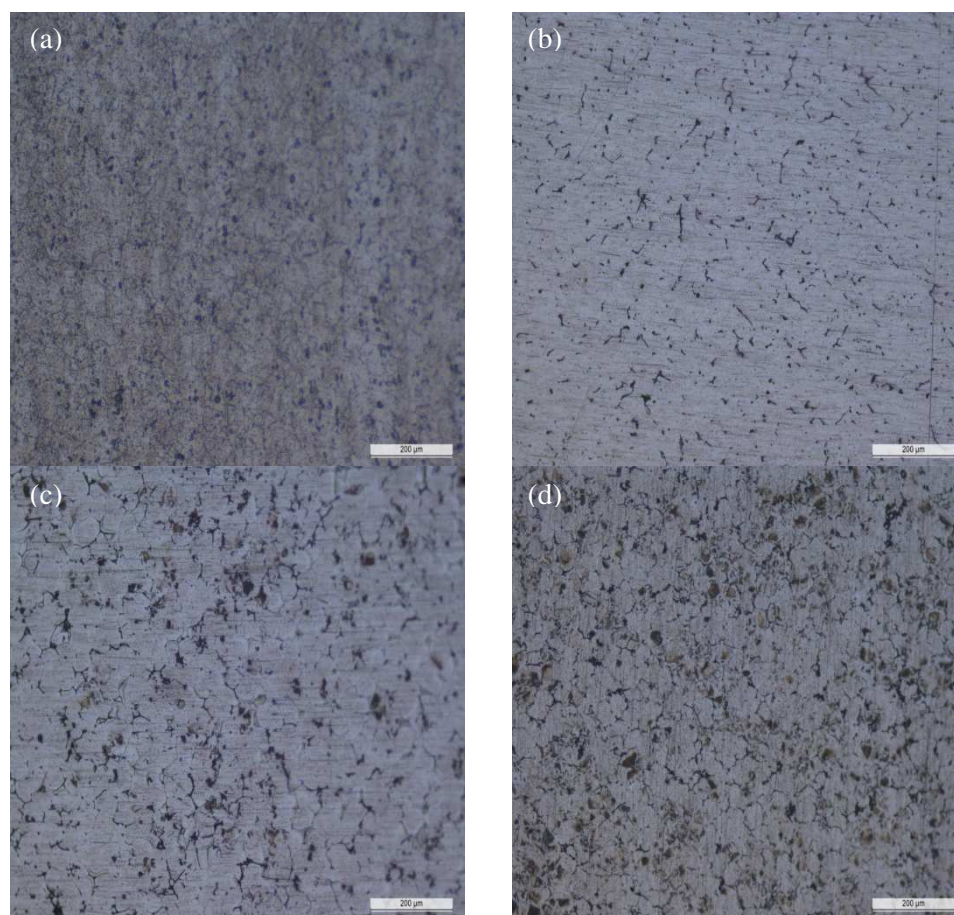


Fig. 7 OM image showing the surface of alloys before corrosion

(a) specimen-1, (b) specimen-2, (c) specimen-3, and (d) specimen-4 alloys.

Fig. 9 presents a high-magnification image of intermetallics and corresponding area map as collected using energy dispersive x-ray spectroscopy (EDS). Presence of Al, Mg and Mn elements observed in Fig.9(a), in addition to Al, Mg, Mn elements, Sc and Zr-containing intermetallic though its peaks not observed from Fig. 9(b)–(d), it is evident from EDS elemental analysis table 2 [19].

Table. 2 SEM-EDS elemental analysis of Al-Mg-Mn-Sc-Zr Alloys

Element	Weight %			
	Specimen-1	Specimen-2	Specimen-3	Specimen-4
Al	94.87	94.28	94.43	94.49
Mg	4.51	4.73	4.47	4.25
Mn	0.62	0.69	0.60	0.56
Sc	–	0.20	0.40	0.60
Zr	–	0.10	0.10	0.10
Totals	100.00	100.00	100.00	100.00

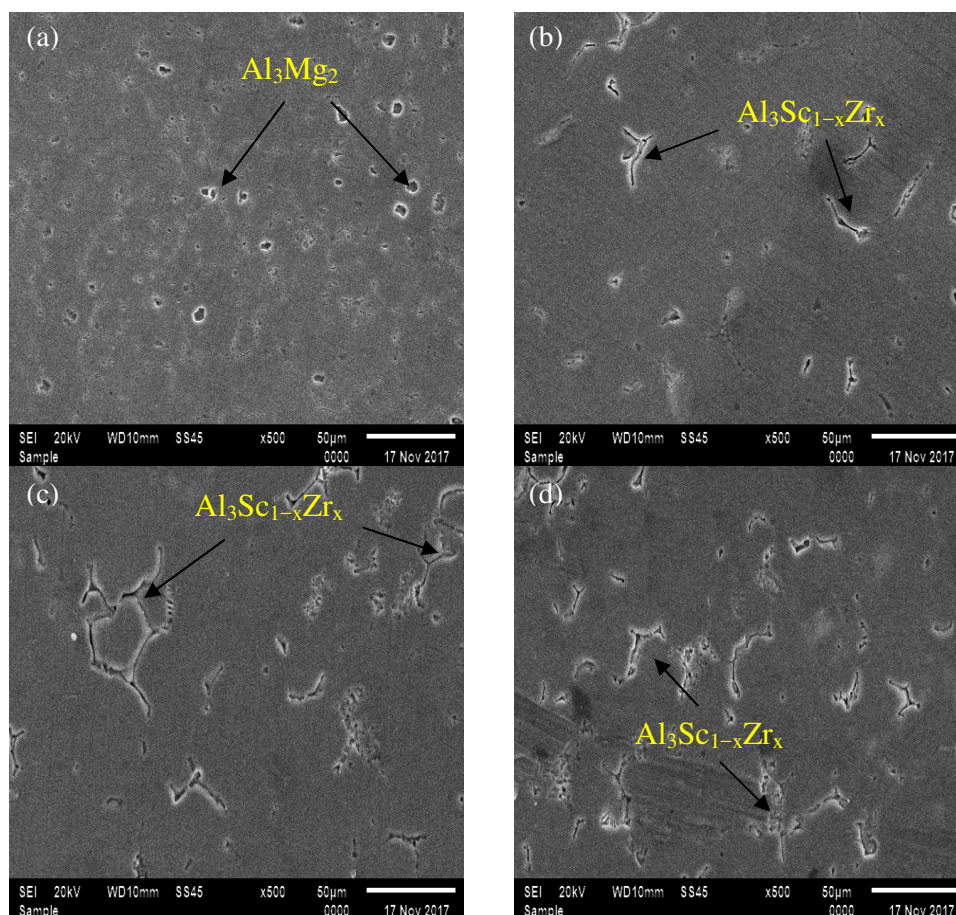
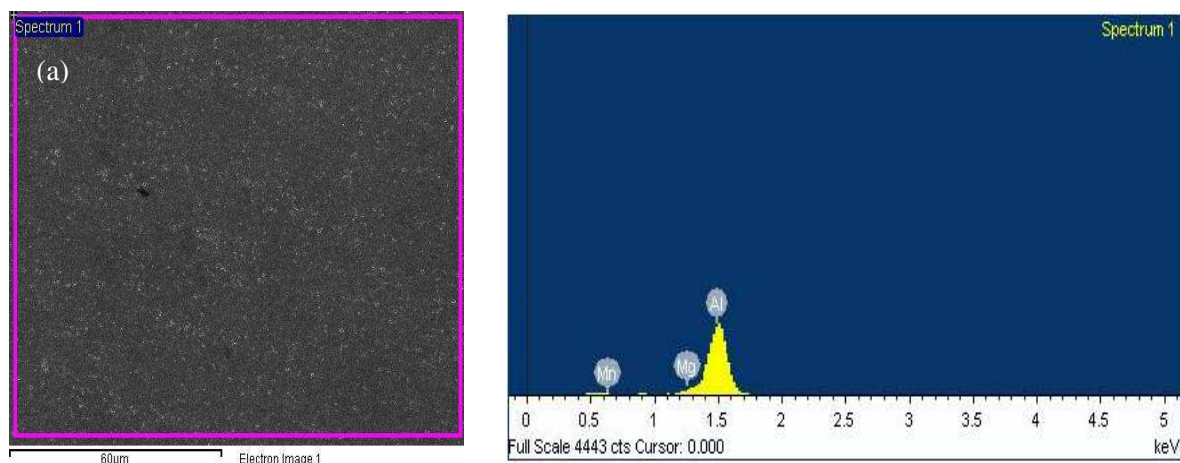


Fig. 8 SEM images showing the surface of alloys before corrosion
(a) specimen-1, (b) specimen-2, (c) specimen-3, and (d) specimen-4 alloys.



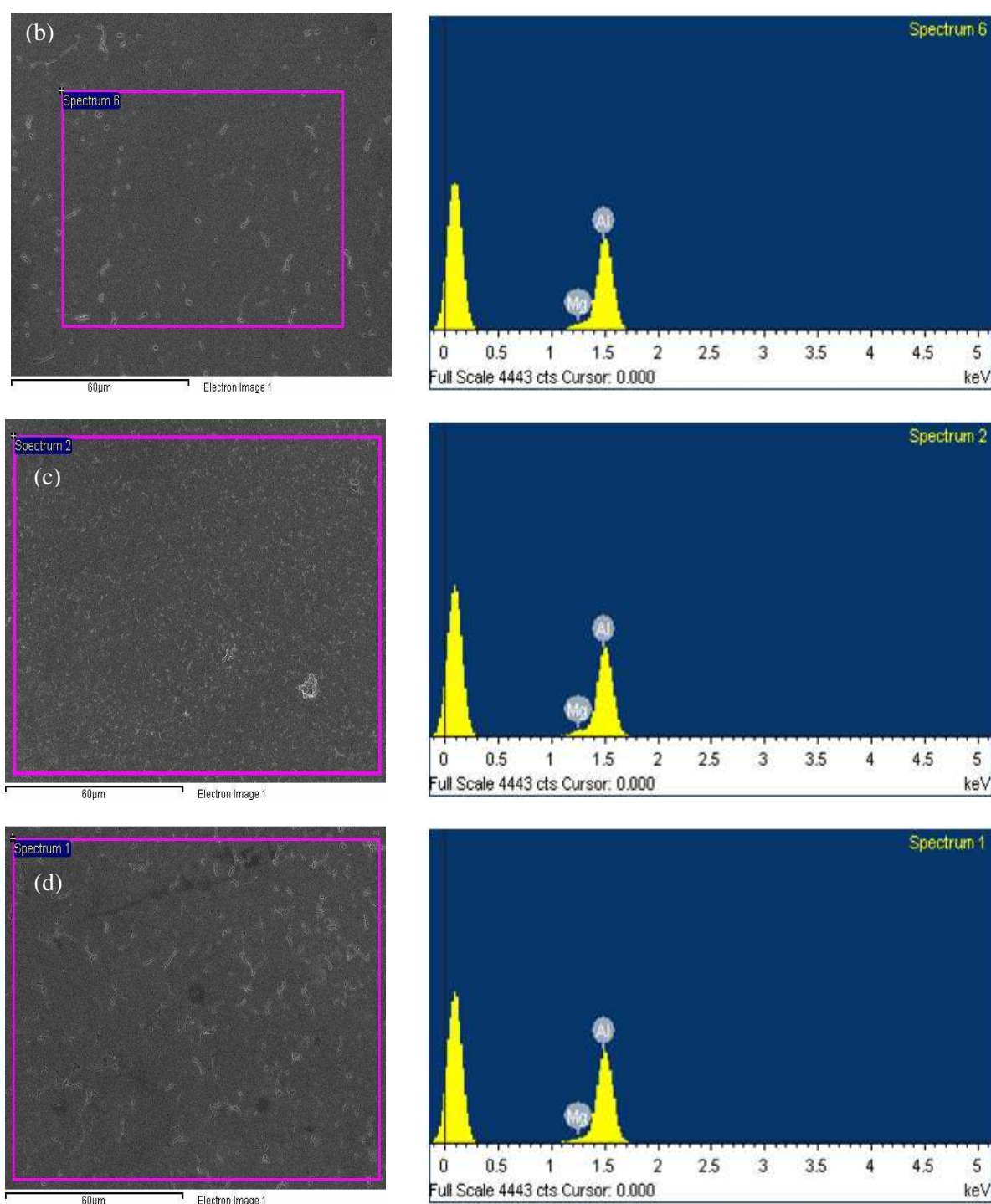


Fig. 9 SEM-EDS image showing the surface of alloys before corrosion
(a) specimen-1, (b) specimen-2, (c) specimen-3, and (d) specimen-4 alloys.

• *X-Ray diffraction Analysis of Al-Mg-Mn-Sc-Zr alloys*

The XRD trace for Al-Mg-Mn-Sc-Zr alloys presented in Fig. 10 confirms the presence of Sc and Zr reinforcement with the Al-Mg-Mn matrix alloy. Sc and Zr containing peaks is observed to be increasing with increment of Sc and Zr content while the Al peak is decreasing [20].

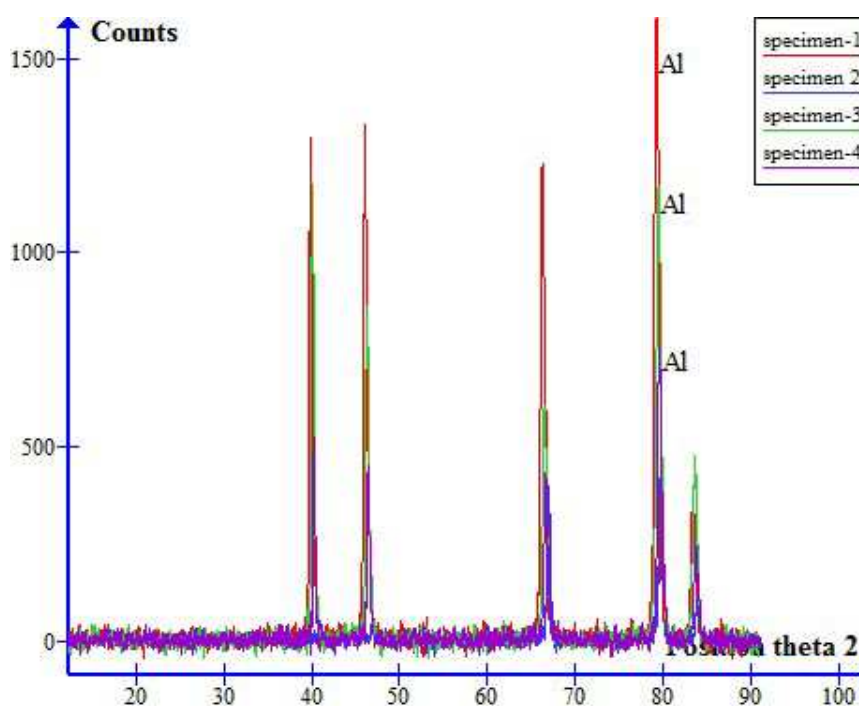


Fig. 10 XRD Patterns

(a) specimen-1, (b) specimen-2, (c) specimen-3, and (d) specimen-4 alloys.

• *Effect of Sc and Zr on corrosion*

The influence of Sc and Zr added Al-Mg-Mn alloy was studied for corrosion resistance. Fig.11 represents the polarization curves of the specimens which were aged for one hour in 3.5% NaCl solution [21]. The corrosion potential obtained from the polarization curves, are summarized in Table 3.

Table. 3 Electrochemical characteristics of alloys polarized in 3.5wt.% NaCl solution

Specimen type	E_{corr} (mv)
specimen-1	-746.13
specimen-2	-715.42
specimen-3	-704.38
specimen-4	-703.97

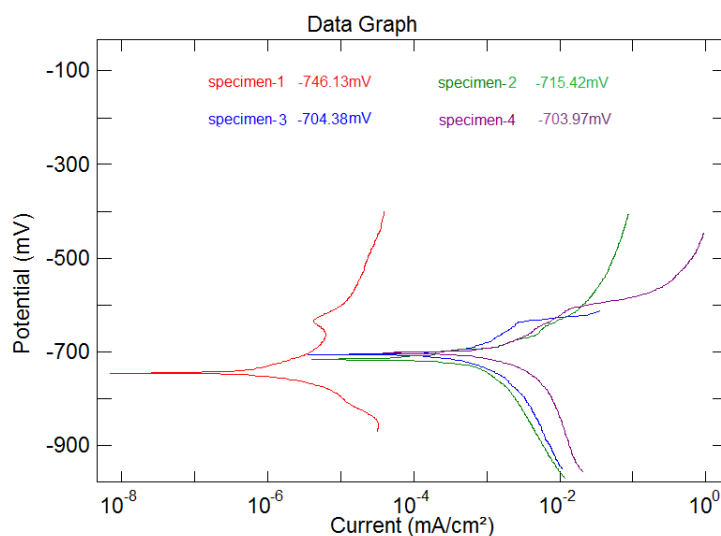


Fig.11 Polarization curves

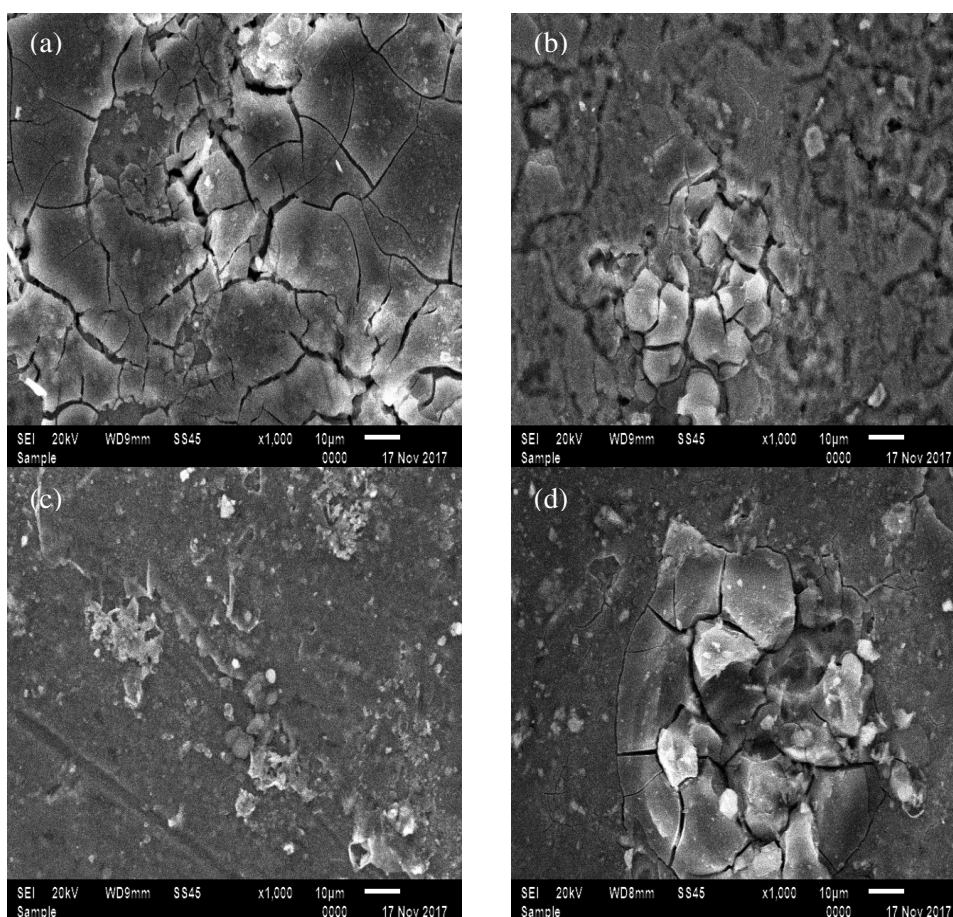
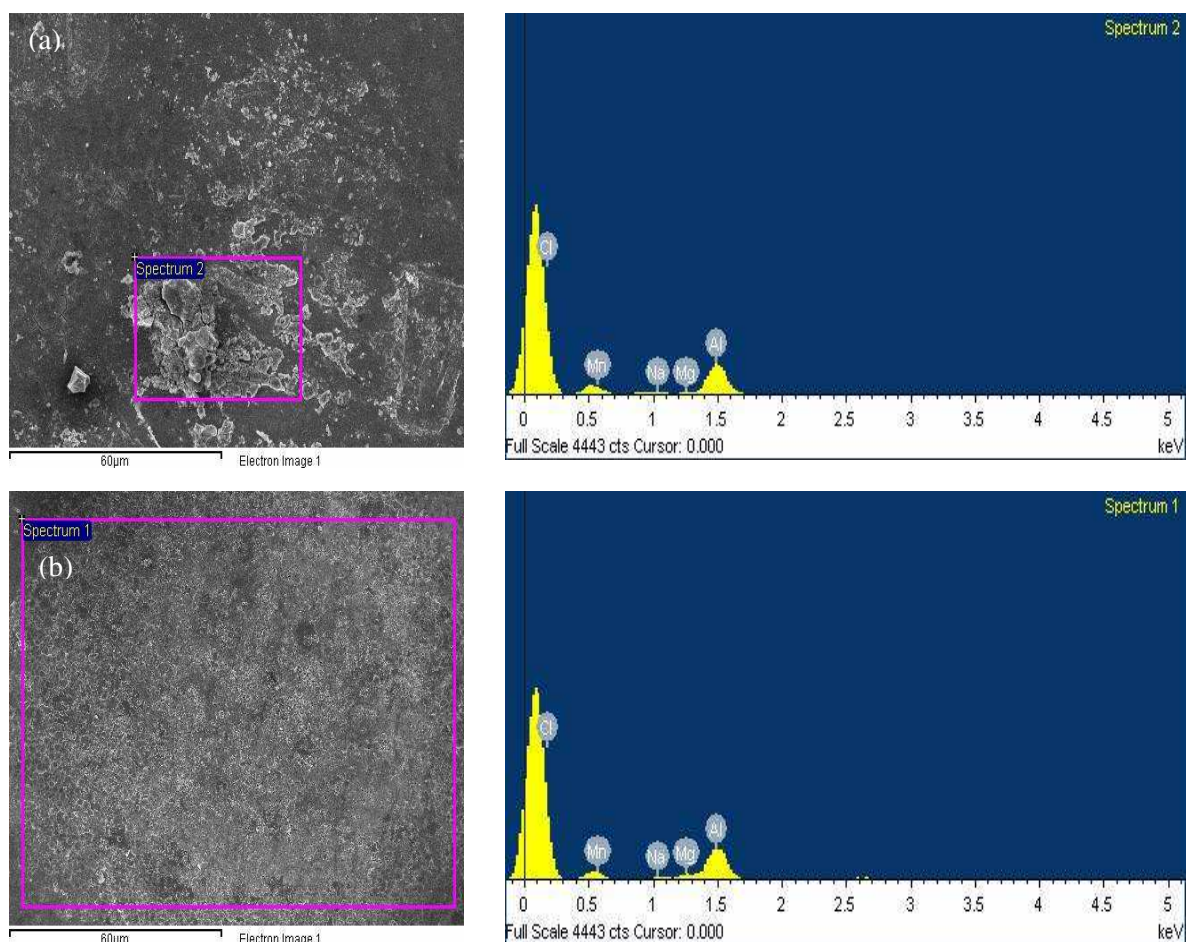


Fig. 12 SEM images of Three-dimensional surfaces of as-rolled
(a) specimen-1, (b) specimen-2, (c) specimen-3, and (d) specimen-4 alloys after corrosion

For corrosion resistance, the electrochemical behavior of the Sc and Zr added Al-Mg-Mn alloys with the Al-Mg-Mn alloy were compared. Anodic dissolution was experienced based on E_{corr} of Al-Mg-Mn alloy. In contrast to this, E_{corr} values in Sc and Zr added Al-Mg-Mn alloys, were experienced less anodic dissolution due to $\text{Al}_3\text{Sc}_{1-x}\text{Zr}_x$ phases [22].

As shown in table 3, the corrosion potential (E_{corr}) of specimen-4 is much lower than those of specimen-1 to specimen-3. Thus, the corrosion susceptibility of the alloys were ranked in the order from high to low as follows: specimen-1, specimen-2, specimen-3, and specimen-4.

Effect of Sc and Zr addition can be observed in the alloy specimens where corrosion damage was observed in the alloy without Sc and Zr (Fig. 12 (a)–(d)). This corrosion damage which was rarely observed in Sc and Zr-containing alloys [23]. SEM observations showed that corrosion occurring in the surrounding area of the Sc and Zr-containing intermetallic phases was minimal, in comparison to that of Al-Mg-Mn intermetallic (Fig. 12).



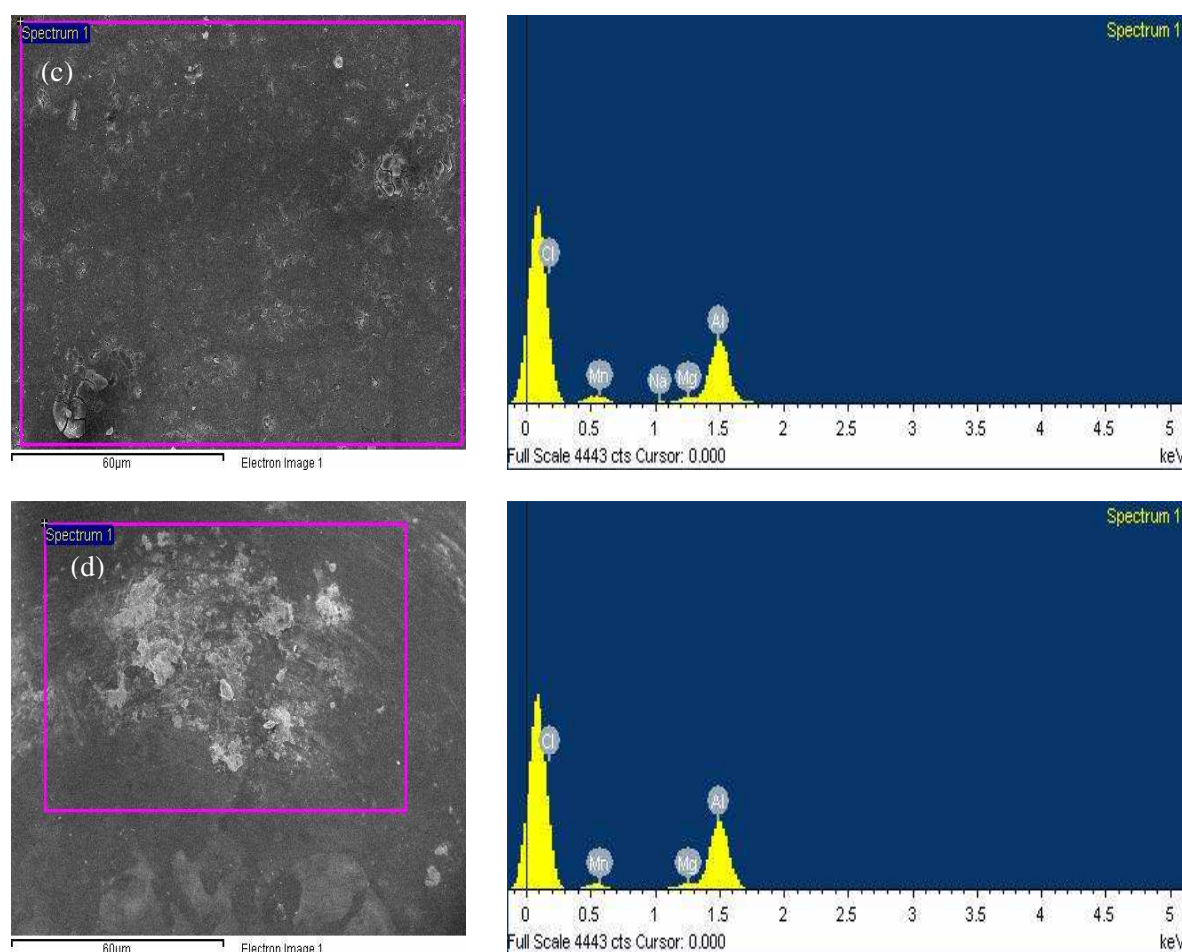


Fig. 13 SEM EDS images of Three-dimensional surfaces of as-rolled (a) specimen-1, (b) specimen-2, (c) specimen-3, and (d) specimen-4 alloys after corrosion.

Table. 5 EDS elemental analysis of Al-Mg-Mn-Sc-Zr Alloys after corrosion

Element	Weight %			
	Specimen-1	Specimen-2	Specimen-3	Specimen-4
Al	92.66	82.19	73.71	86.85
Mg	6.70	4.57	11.16	6.56
Mn	0.64	1.27	1.55	1.73
Sc	–	1.38	1.86	1.39
Zr	–	0.56	0.67	0.13
Na	–	5.93	6.21	2.25
Cl	–	4.11	4.83	1.10
Totals	100.00	100.00	100.00	100.00

Localized corrosion attack was very less due to Sc and Zr which were observed in the elemental analysis using SEM EDS [23–24]. Therefore, the morphology of the surfaces and corrosion occurring around intermetallic phases after corrosion test were observed using SEM EDS (Fig. 13(a)–(d)). Table 5 shows the EDS elemental analysis of Al–Mg–Mn–Sc–Zr Alloys after corrosion.

Conclusions

On the basis of the results obtained from the investigations, the following are the main conclusions:

- i. Al–Mg–Mn–Sc–Zr alloys were successfully fabricated by stir casting technique.
- ii. Minor additions of 0.2 – 0.6 wt. % scandium and 0.1wt. % Zr introduces a relatively high level of strength in Al–Mg–Mn as shown by the improvement in hardness.
- iii. Vickers hardness measurement shows a gradual increase of hardness was observed with its peak at specimen–3, and then decreased afterwards.
- iv. Microstructural and characterisation of Al–Mg–Mn–Sc–Zr alloy confirmed the appearances of Al_3Sc and spherical $\text{Al}_3\text{Sc}_{1-x}\text{Zr}_x$ particles and their growth in association with minor additions of 0.2 – 0.6 wt. % scandium and 0.1wt. % Zr.
- v. Scandium (0.2–0.6 wt. %) and Zirconium (0.1wt.%) addition introduce an appreciable increase in the corrosion resistance of Al–Mg–Mn alloys.

References

- [1] M. Kciuk, Structure, mechanical properties and corrosion resistance of AlMg5 alloy, *Journal of Achievements in Materials and Manufacturing Engineering* 17 pp.185–188, (2006).
- [2] M. Kciuk, S. Tkaczyk, Structure, mechanical properties and corrosion resistance of AlMg5 and AlMg1Si1 alloys, *Journal of Achievements in Materials and Manufacturing Engineering* 21 /1 pp.39–42, 2007.
- [3] A. Atkowski, M. Branicki, Thermo–mechanical treatment of non–ferrous metal alloys, AGH Publishing House, Cracow, 1981.
- [4] M.M. Sharma, M. F. Amateau, T.J. Eden, Aging response of Al–Zn–Mg–Cu spray formed alloys and their metal matrix composites, *Material Science and Engineering A* 424 (2006) pp.87–96.
- [5] K. B. Hyde, A. F. Norman and P. B. Prangnell: ‘The effect of cooling rate on the morphology of primary Al_3Sc intermetallic particles in Al–Sc alloys’, *Acta Mater.*, 2001, 49, 1327–1337.

- [6] L. L. Rokhlin, T. V. Dobatkina and M. L. Kharakterova: 'Structure of the phase equilibrium diagrams of aluminum alloys with scandium', *Powder Metall. Met. C*, 1997, 36C, 128-132.
- [7] F. Jiang, J. Zhou, H. Huang and J. Qu, "Characterisation of microstructure and mechanical properties in Al-Mg alloy with addition of Sc and Zr" *Materials Research Innovations* 2014 Vol 18 suppl 4 S4-228-234
- [8] Lowell A. Willey, US Patent NQ 3619181, Nov. 9, 1971.
- [9] V.I. Yelagin, V.V. Zakharov, T.D. Rostova, Tsvetnye metally 12 (1982) 96-99.
- [10] Sumiha Ikeshita, Ansis Strodahs, Zineb Saghi, Kazuhiro Yamada, Pierre Burdet, Satoshi Hata, Ken-ichi Ikeda,1, Paul A. Midgley, Kenji Kaneko," Hardness and microstructural variation of Al-Mg-Mn-Sc-Zr alloy" *Micron* 82 (2016) pp.1-8.
- [11] Ikeshita, S., Strodahs, A., Saghi, Z., Yamada, K., Burdet, P., Hata, S., Ikeda, K.-I., Midgley, P.A., Kaneko, K., 2016. Hardness and microstructural variation of Al-Mg-Mn-Sc-Zr alloy. *Micron* pp.82, 1-8.
- [12] Vlach, M., Stulikova, I., Smola, B., Kekule, T., Kudrnova, H., Danis, S., Gemma, R., Ocenasek, V., Malek, J., Tanprayoon, D., Neubert, D., 2013. Precipitation in coldrolled Al-Sc-Zr and Al-Mn-Sc-Zr alloys prepared by powder metallurgy. *Mater. Charact.* 86, pp.59-68.
- [13] M.S. Kaiser and M.K. Banerjee "Effect of Ternary Scandium and Quaternary Zirconium and Titanium Additions on the Tensile and Precipitation Properties of Binary Cast Al-6Mg Alloys" *Jordan Journal of Mechanical and Industrial Engineering*, Volume 2, Number 2, Jun. 2008, ISSN 1995-6665, Pages 93 - 99.
- [14] Zaki Ahmad Anwar Ul-Hamid and Abdul-Aleem B.J." The corrosion behaviour of scandium alloyed Al 5052 in neutral sodium chloride solution" *Corrosion Science* 43 (2001) 1227-1243.
- [15] Yudai Miyake, Yukio Sato, Ryo Teranishi, Kenji Kaneko,' Effect of heat treatments on the microstructure and formability of Al-Mg-Mn-Sc-Zr alloy', *Micron* 101 (2017) pp.151-155.
- [16] S.Lathabai,; P.G. Lloyd, "Effect of scandium on the microstructure, mechanical properties and weldability of cast Al-Mg alloys. *Acta materialia*. 2002 journal ISSN : 1359-6454 ; 50(17): 4275-4292.
- [17] TadashiAiura, NobutakaSugawara, YasuhiroMiura, "The effect of scandium on the as-homogenized microstructure of 5083 alloy for extrusion" *Materials Science and Engineering: A*, Volume 280, Issue 1, 15 March 2000, Pages 139-145.
- [18] V.G. Davydov, T.D. Rostova, V. V. Zakharov, Yu. A. Filatov, V. I. Yelagin," Scientific principles of making an alloying addition of scandium to aluminium alloys", *Materials Science and Engineering A* 280 (2000) pp.30-36.

- [19] ZhiminYin, QinglinPan, YonghongZhang, FengJiang "Effect of minor Sc and Zr on the microstructure and mechanical properties of Al–Mg based alloys" *Materials Science and Engineering: A*, Volume 280, Issue 1, 15 March 2000, Pages 151–155.
- [20] A.F Norman, KHyde, FCostello, SThompson, SBirley, P.BPrangnell, "Examination of the effect of Sc on 2000 and 7000 series aluminium alloy castings: for improvements in fusion welding" *Materials Science and Engineering: A*, Volume 354, Issues 1–2, 15 August 2003, Pages 188–198
- [21] N. Birbilis ,Z and R. G. Buchheit, "Electrochemical Characteristics of Intermetallic Phases in Aluminum Alloys" *Journal of The Electrochemical Society*, 152 (4) B140–B151 (2005).
- [22] ASTM: Recommended Practice G5–87 for Making Potentiostatic and Potentiodynamic Polarization Measurement, Annual Book of Standards, vols. 3 and 2, Part 10, 1998.
- [23] Kannan M B, Raja V S. Influence of heat treatment and scandium addition on the electrochemical polarization behavior of Al–Zn–Mg–Cu–Zr (7010) alloy [J]. *Metallurgical and Materials Transactions A*, 2007, 38: pp.2843–2852.
- [24] Chen K H, Fang H C, Zhang Z, Chen X, Liu G. Effect of of Yb, Cr and Zr additions on recrystallization and corrosion resistance of Al–Zn–Mg–Cu alloys [J]. *Materials Science and Engineering A*, 2008, 497: pp.426–431.